

# A test of Radial Acceleration Relation for the *Giles et al Chandra* cluster sample

S. Pradyumna\* and Shantanu Desai†

*Department of Physics, Indian Institute of Technology, Hyderabad, Telangana-502285, India*

We carry out a test of the radial acceleration relation (RAR) for a sample of 10 dynamically relaxed and cool-core galaxy clusters imaged by the Chandra X-ray telescope, which was studied in [1]. For this sample, we observe that the best-fit RAR shows a very tight residual scatter equal to 0.09 dex. We obtain an acceleration scale of  $1.59 \times 10^{-9} m/s^2$ , which is about an order of magnitude higher than that obtained for galaxies. Furthermore, the best-fit RAR parameters differ from those estimated from some of the previously analyzed cluster samples, which indicates that the acceleration scale found from the RAR could be of an emergent nature, instead of a fundamental universal scale.

## I. INTRODUCTION

Three recent works [2–4] have studied disparate samples of galaxy clusters, in order to ascertain if they obey the Radial Acceleration relation (RAR). The RAR is a tight correlation between the baryonic ( $a_{bar}$ ) and the total dynamical acceleration ( $a_{tot}$ ). A first definitive case for the RAR was asserted using the SPARC sample consisting of spiral galaxies [5], who showed the RAR is obeyed with a scatter of 0.13 dex, with most of this scatter been attributed to observational uncertainties [6]. The RAR, which was deduced from the SPARC sample can be written as follows:

$$a_{tot} = \frac{a_{bar}}{1 - e^{-\sqrt{a_{bar}/a_0}}}, \quad (1)$$

where  $a_0 \sim 1.2 \times 10^{-10} m/s^2$  [5]. However, some objections to  $a_0$  been a fundamental universal constant (valid for all galaxies) have been raised [7–10]. Ref. [7] showed that the presence of a fundamental acceleration scale is ruled out at more than  $10\sigma$ , and there is no value of  $a_0$  which is compatible within  $5\sigma$  for all galaxies. This work concluded that the RAR is an emergent one, which arises after stacking the data from a large number of galaxies. There is an ongoing debate on these issues [8–12]. Most recently, the results in [7] were also confirmed in [10, 13]. (See also Ref. [14]).

More generally, the RAR can be re-written as a linear regression relation between the logarithms of  $a_{bar}$  and  $a_{tot}$ ,  $\ln(a_{tot}) = m \ln(a_{bar}) + b$ . All RAR studies for clusters have been obtained by carrying out this linear regression between these two accelerations in logarithmic space [2]. This relation can be trivially deduced from Milgrom’s MOND paradigm [15]. However, the observed tight scatter cannot be trivially predicted by the standard  $\Lambda$ CDM model [16–18] (see also the discussion in [19]). However, if  $a_0$  is of emergent nature, as argued in [7, 10], then the RAR could be reproduced from the complex interplay between dark matter and baryons [17, 18, 20],

including the effects due to the adiabatic contraction of dark in the presence of baryons [21].

We have been knowing for more than three decades that MOND does not work for relaxed galaxy clusters [22, 23] (and references therein). Furthermore, relativistic MOND theories cannot explain the coincident GW-EM signal [24] as well as large-scale structure probes [25]. However, a detailed characterization of the RAR in galaxy clusters could be an invaluable probe, that could be used to adjudicate between various alternatives to the standard  $\Lambda$ CDM model, which can reproduce the success of Milgrom’s MOND’s paradigm, but are consistent with  $\Lambda$ CDM predictions at larger scales from CMB [26].

Motivated by these considerations, three different groups recently carried out a test of the RAR for multiple galaxy cluster samples [2–4]. They have found that the residual scatter between the observed data and best-fit RAR is between 0.11-0.13 dex (see Table I of [4] for a summary). However, the aforementioned works have found that the acceleration scale  $a_0$  in Eq. 1 is  $\mathcal{O}(10^{-9}) m/s^2$ , which is about an order of magnitude larger than that obtained for rotationally supported galaxies [5]. Most recently, this work has also been extended to galaxy groups [27], who find that the scatter is larger, and  $a_0$  falls in-between single galaxies and clusters.

Given the importance of RAR as a probe of  $\Lambda$ CDM and its alternatives, it is important to cross-check these results with more cluster samples to gain further insight on how universal this relation is for clusters, and whether there are any exceptions. In the past three decades a large number of dedicated X-ray based cluster surveys using ROSAT, Chandra, and XMM-Newton (along with other multi-wavelength data) have used the observed cluster samples to address a plethora of science goals in Cosmology, galaxy evolution, and fundamental Physics [28, 29]. The same data can also be used for precision tests of RAR.

In this work, we therefore carry out another test of RAR with one such galaxy cluster sample studied in [1], which we refer to as Giles et al cluster sample. This sample has been recently used to test Verlinde’s Emergent gravity paradigm [30]. The outline of this manuscript is as follows. The basic methodology used for our analysis is

\*E-mail: ep18btech11015@iith.ac.in

†E-mail: shntn05@gmail.com

described in Sect. II. The Giles et al cluster sample along with our data analysis procedure is outlined in Sect. III. Our results are described in Sect. IV. We conclude in Sect. V.

## II. BASIC CLUSTER PHYSICS

We now provided an abridged description of all the ingredients necessary to carry out a test of RAR using clusters. More details can also be found in our past works [4, 27, 31].

Galaxy clusters are the largest gravitationally collapsed objects in the universe [29]. Most of their mass ( $\sim 85\%$ ) comprises dark matter, whereas most of the remaining baryonic mass resides in the form of diffuse hot gas ( $\sim 13\%$ ) in the Intra-Cluster Medium (ICM). Only a small fraction of the baryonic mass ( $\sim 2\%$ ) is in the form of stars. At X-Ray wavelengths, the hot ICM emits via thermal bremsstrahlung [28]. The total mass of a cluster can be estimated from X-Ray measurements assuming that the ICM is in hydrostatic equilibrium within the gravitational potential of the cluster. The total acceleration for test particles in hydrostatic equilibrium within a gravitational potential is given by [28, 32]:

$$a_{tot}(r) = -\frac{k_b T}{r \mu m_p} \left( \frac{d \ln \rho_{gas}}{d \ln r} + \frac{d \ln T}{d \ln r} \right), \quad (2)$$

Here,  $a_{tot}$  is the dynamic acceleration of the cluster as a function of radius from the cluster center ( $r$ ),  $k_b$  is the Boltzmann constant,  $T$  is the parametrized temperature,  $\rho_{gas}$  is the parametrized density of the gas,  $\mu m_p$  is the mean molecular weight. We use a  $\mu$  value of 0.6 resulting in  $\mu m_p \approx 10^{-27}$  kg. The hydrostatic equilibrium equation is applicable for relaxed clusters. Once we know the total mass we can estimate the total acceleration ( $a_t$ ) from Newtonian gravity.

Now, for estimating the acceleration due to baryons, we need to estimate the gas mass ( $M_{gas}$ ) and the stellar mass ( $M_{star}$ ). The gas density ( $\rho_{gas}$ ) profiles are estimated and modelled using the observed projected X-ray emissivity profile. Assuming spherical symmetry, we can derive the gas mass  $M_{gas}$  using:

$$M_{gas} = \int 4\pi r^2 \rho_{gas}(r) dr \quad (3)$$

It should be noted that the aforementioned calculations of gas and total mass assume spherical symmetry. The uncertainty associated with this assumption is about 5% (See [31] and references therein). For stellar mass, we use the empirical relation obtained in [33], which gives the stellar mass at  $R_{500}$ , where  $R_{500}$  is the radius at which the overdensity is 500 times the critical density of the universe, i.e.  $\rho(R_{500}) = 500 \left( \frac{3H^2}{8\pi G} \right)$ . The total star mass  $M_{star}(R_{500})$  at  $R_{500}$  is given by:

$$\frac{M_{star}(R_{500})}{10^{12} M_{\odot}} = 1.8 \left( \frac{M_{500}}{10^{14} M_{\odot}} \right)^{0.71} \quad (4)$$

Then, to estimate the stellar mass at any other radius ( $r$ ), we assume that the stellar component follows an isothermal distribution, and we thereby obtain [34]:

$$M_{star}(r) = \left( \frac{r}{R_{500}} \right) M_{star}(R_{500}) \quad (5)$$

The baryonic acceleration ( $a_b$ ) can then be obtained at any value of the radius  $r$  from the sum of the gas and star mass.

## III. DATA AND ANALYSIS:

Giles et al [1] (G17, hereafter) provide the temperature and gas density profile fits for 34 clusters within the redshift range  $0.15 \leq z \leq 0.3$ , which were imaged with the Chandra X-ray telescope. The main goal of this work was to characterize the scatter in the Luminosity-Mass relation for this sample. This cluster sample was selected from the ROSAT based Brightest cluster sample survey [35, 36] with a lower luminosity cutoff of  $L_X$  ( $0.1-2.4$  keV)  $\geq 6 \times 10^{44}$  erg/sec [37]. This cut provided a sample of 36 clusters. From these, A689 was culled because of data quality issues and Zw5768 did not pass the luminosity cut using a revised redshift estimate. The exposure times for these clusters are in the range of 7.3-450 ks (cf. Table 1 of G17). The luminosity of these clusters in X-Ray band of 0.1-2.4 keV falls between  $\sim (6.3-24.5) \times 10^{44}$  erg/s. More details of the observations and data reduction can be found in G17.

Since hydrostatic equilibrium can be robustly used to obtain the mass only if the cluster is dynamically relaxed and has a cool core, we select a sub-sample of relaxed as well as cool core clusters for our analysis. This was done in two steps: (1) the clusters were determined to be in a relaxed or non-relaxed state, on the basis of the centroid shift ( $\langle w \rangle$ ) [38], the description of which can be found G17; (2) the cluster sample was further bifurcated into cool core and non-cool core sample. A cut of  $\langle w \rangle < 0.009 r_{500}$  was made to select dynamically relaxed clusters. The presence of a cool core was based on the calculating the central cooling time given by:

$$t_{cool}(yr) = 8.5 \times 10^{10} \left( \frac{n_p}{10^{-3}} \right)^{-1} (0.079 k T_{CCT})^{1/2}$$

The last parameter used for the selection of cool core sample was the cuspieness, which is defined as the logarithmic slope of gas density at  $0.04 r_{500}$  [39]. In summary, cuts were applied on  $\langle w \rangle < 0.009 r_{500}$ ,  $t_{cool} < 7.7 Gyr$ , cuspieness  $> 0.7$ , to select the dynamically relaxed and cool core sample. After applying these cuts, we are left with a sample of 10 clusters (from the original dataset of 34 clusters) for our

analysis. They are: A2204, RXJ1720.1+2638, A1423, Z2089, RXJ2129.6+0005, A1835, MS1455.0+2232, RXJ0439.0+0715, RXJ0437.1+0043, Z3146.

The gas density ( $\rho_{gas}$ ) model used is equal to  $1.624m_p\sqrt{n_p(r)n_e(r)}$ , where  $m_p$  is the proton mass;  $n_p$  and  $n_e$  are the proton and electron number densities, respectively. Their product ( $n_en_p$ ) is parametrized by a modified single- $\beta$  profile:

$$n_e(r)n_p(r) = \frac{(r/r_c)^{-\alpha}}{(1+r^2/r_c^2)^{3\beta-\alpha/2}} \frac{n_0^2}{(1+r\gamma/r_s^\gamma)^{\epsilon/\gamma}} \quad (6)$$

This is a variant of the double- $\beta$  profile used by Vikhlinin et al [40], which was also used in our previous works [4, 31, 41, 42]. The second term in the double- $\beta$  profile was dropped so as to fit both the low and high quality data in the sample.

The temperature profile used for our current analysis is:

$$T(r) = T_0 \frac{(x + T_{min}/T_0)}{x + 1} \frac{(r/r_t)^{-a}}{[1 + (r/r_t)^b]^{c/b}}, \quad (7)$$

where  $x = \left(\frac{r}{r_{cool}}\right)^{a_{cool}}$ . The values of the free parameters in Eq. 7 for these clusters can be found in Table A2 of G17. The error estimates for the temperature and density have been obtained in G17 using Monte-Carlo simulations. For this work, the temperature error bars used in our analysis have been obtained by digitization of the plots in G17, which in turn were used to propagate the errors in  $M_{tot}$ . For the errors on the gas density, we again digitized the emission measure plots given in G17. We calculated the fractional errors in the emission measure data at the radii of interest by using *spline* interpolation. Then using the fact that the gas density is proportional to the square root of the emission measure, the fractional error in the density is given as:  $\frac{\Delta\rho_{gas}}{\rho_{gas}} = \frac{1}{2} \frac{\Delta EM}{EM}$  where EM stands for the emission measure value. We now plug in the values for  $\rho(r)$  and  $T(r)$  from Eqns. 6 and 7 respectively in Eq. 2 to calculate the total dynamical acceleration  $a_{tot}(r)$ .

To estimate baryonic mass, we need to determine the gas and star mass. The gas mass can be estimated from the gas density profile in Eq. 6. To estimate the stellar mass, we need  $R_{500}$  and  $M_{500}$  for these clusters. G17 provides these  $R_{500}$  estimated using the hydrostatic mass estimates. We plugged these values in Eq. 4 to obtain the total stellar mass estimate at  $R_{500}$ . The stellar mass at all other radii was obtained from Eq. 5. Therefore, the baryonic acceleration can then be estimated from this total baryonic mass assuming Newtonian gravity.

Now, we do a joint fit to the RAR using the calculated data along with associated errors for  $a_{tot}$  and  $a_{bar}$  at  $r = 100, 200, 400,$  and  $600$  kpc for all the clusters. The only exception is Z2089, for which we used measurements at 100, 200, 400, and 560 kpc. Similar to previous works [2, 4], we do a fit in log-acceleration space by doing a linear regression to the relation:

$$y = mx + b \quad (8)$$

where  $y = \ln(a_{tot})$  and  $x = \ln(a_{bar})$ . We then maximize a log-likelihood given by :

$$-2 \ln L = \sum_i \ln 2\pi\sigma_i^2 + \sum_i \frac{[y_i - (mx_i + b)]^2}{\sigma_i^2} \quad (9)$$

$$\sigma_i^2 = \sigma_{y_i}^2 + m^2\sigma_{x_i}^2 + \sigma_{int}^2 \quad (10)$$

Here,  $\sigma_{y_i}$  and  $\sigma_{x_i}$  denote the errors in  $y$  and  $x$  respectively;  $\sigma_{int}$  is the intrinsic scatter for our linear relation between the logarithms of the accelerations, which is a free parameter. We used the `emcee` MCMC sampler [43] to sample the likelihood in Eq. 9. The total number of steps and burn-in steps used for the MCMC analysis are 3000 and 500 respectively. The number of walkers used for our MCMC analysis is equal to 40. We used uniform non-informative priors on  $m$ ,  $b$ , and  $\ln(\sigma_{int})$  given by:  $m \in [-10, 10]$ ;  $b \in [-100, 100]$ ; and  $\ln(\sigma_{int}) \in [-5, -1]$ .

For calculating the residual scatter in dex, we first calculate residuals by subtracting the  $\log_{10}(a_{dyn})$  predicted by our best-fit from  $\log_{10}(a_{dyn})$  calculated from the data. This is the same practise used in the literature to characterize the scatter in the RAR [4]. We then fit a normal distribution with a mean of zero to these residuals. The standard deviation obtained is used to characterize the residual scatter in dex.

## IV. RESULTS

We now present the results of our analysis of 10 relaxed cool core clusters from this sample. Fig. 1 shows the best-fit line obtained for the data along with the best fits obtained by McGaugh et al [5] (for galaxies), Tian et al [2], Chan and Del Popolo [3] and our previous analysis [4] (on galaxy clusters). Fig 2 shows the 68% and 95% credible intervals for the slope, intercept, and the natural log of intrinsic scatter obtained using the *ChainConsumer* post-processing package [44], using the MCMC chains from `emcee` as inputs. The best-fit slope and intercept obtained are  $m = 1.03 \pm 0.05$  and  $b = 2.7^{+1.3}_{-1.2}$  respectively. The residual scatter obtained for the best fit is about 0.08 dex. The best-fit values and the scatter are shown in Table I alongside the fits obtained in previous works for comparison. We note that the best-fit slope and intercept observed for XCOP sample and the current sample agree within  $1\sigma$ . However, the best-fit parameters of the G17 sample differ from the other cluster samples, such as the Vikhlinin et al Chandra sample [40], HIFLUGS sample [3], and the CLASH sample [2] to between  $3 - 5\sigma$ . The acceleration scale that we obtain for current sample on fixing the slope to  $m = 0.5$  is equal to  $(1.59 \pm 0.14) \times 10^{-9} m/s^2$ . The error in  $a_0$  was estimated using error propagation, based on the  $1\sigma$  error in  $b$ , which was obtained from redoing the RAR fit for a fixed slope of 0.5. The acceleration scale obtained for this sample of galaxy clusters is therefore, an order of magnitude higher than the  $a_0$  obtained from the SPARC

sample [5] for galaxies, in agreement with all previous analyses carried out on galaxy clusters. [2–4].

When we try to apply a cut to look for dynamically relaxed but non-cool clusters, using only the dynamically relaxed criteria mentioned in Sec III, we find three additional clusters for our analysis. Then, we tried to do a similar analysis on all the relaxed clusters (both cool core and non-cool core). The best fit slope and intercept obtained in this case are  $m = 0.92 \pm 0.07$  and  $b = 0.0 \pm 1.7$ , and the scatter increases slightly to 0.095 dex.

Therefore, our results reinforce those in our previous work, and indicate the RAR is obeyed for clusters with a tight intrinsic scatter. However, this relation is not universal, as all the cluster samples do not agree on the RAR best-fit parameters. These inconsistent fits among the different cluster samples, reaffirm the view that  $a_0$  could be of emergent nature, instead of a fundamental acceleration scale, as previously discussed [7, 10].

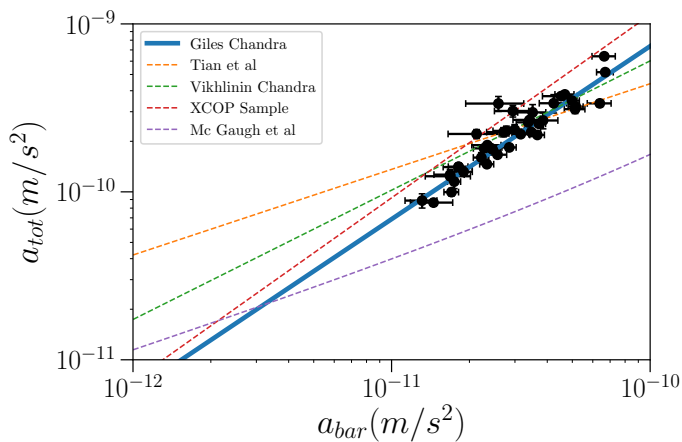


FIG. 1: The best-fit RAR (blue solid line) obtained for  $a_{tot}$  vs  $a_{bar}$  data for a sample of 10 dynamically relaxed and cool-core galaxy clusters from the G17 catalog. Best fits from previous works on RAR for clusters have been overlaid for comparison.

## V. CONCLUSIONS

We implement a test of the scatter in the correlation between the total dynamical and baryonic acceleration

in log-log space (dubbed as RAR) using a sample of 10 dynamically relaxed cool core clusters, obtained from a dataset of 35 ROSAT selected clusters imaged with Chandra, and described in detail in G17. The aim of this work was to further assess the conclusions of previous studies of RAR using ancillary cluster samples [2–4]. These previous analyses showed that the intrinsic scatter of the RAR is the same as that seen for spiral galaxies [5], but the observed acceleration scale is elevated by an order of magnitude, and the best-fit values are inconsistent among the cluster samples [4].

The best-fit values for the parameters of the RAR using the G17 cluster sample can be found in Fig. 2. The best-fit RAR along with the data is shown in Fig. 1. A comparison of our best-fit results along with those from the previous works is summarized in Table I. We find that the scatter for this sample is equal to 0.08 dex and is slightly increased to 0.094 dex, once we include the relaxed non-cool core clusters. Our estimate for the acceleration scale we obtained by positing a slope of 0.5 in the RAR regression relation is about an order of magnitude larger than that deduced using the SPARC sample. The best-fit value for the slope and intercept is in agreement with the same for the XCOF sample, but differ from other cluster samples previously analyzed by upto  $5\sigma$ . This shows that the RAR is not universal for clusters. Therefore, this reinforces the fact alluded to in [7, 10], that the acceleration scale deduced from RAR is not a fundamental universal constant, but instead could be an emergent effect caused by stacking data from different clusters.

## Acknowledgments

We would like to thank Paul Giles for useful correspondence about G17. We are also grateful to the anonymous referee for useful feedback on the manuscript.

- 
- [1] P. A. Giles, B. J. Maughan, H. Dahle, M. Bonamente, D. Landry, C. Jones, M. Joy, S. S. Murray, and N. van der Pyl, *Mon. Not. R. Astron. Soc.* **465**, 858 (2017), 1510.04270.
  - [2] Y. Tian, K. Umetsu, C.-M. Ko, M. Donahue, and I. N. Chiu, *Astrophys. J.* **896**, 70 (2020), 2001.08340.
  - [3] M. H. Chan and A. Del Popolo, *Mon. Not. R. Astron. Soc.* p. 218 (2020), 2001.06141.
  - [4] S. Pradyumna, S. Gupta, S. Seeram, and S. Desai, *Physics of the Dark Universe* **31**, 100765 (2021), 2011.06421.
  - [5] S. S. McGaugh, F. Lelli, and J. M. Schombert, *Phys. Rev. Lett.* **117**, 201101 (2016), 1609.05917.
  - [6] P. Li, F. Lelli, S. McGaugh, and J. Schombert, *Astron. & Astrophys.* **615**, A3 (2018), 1803.00022.
  - [7] D. C. Rodrigues, V. Marra, A. del Popolo, and Z. Davari, *Nature Astronomy* **2**, 668 (2018), 1806.06803.
  - [8] D. C. Rodrigues, V. Marra, A. Del Popolo, and Z. Davari,



Cluster Sample	Slope	Intercept	Intrinsic scatter	$a_0$ ( $m/s^2$ )	Scatter (dex)
Giles Chandra (this work)	$1.03^{+0.05}_{-0.05}$	$2.7^{+1.3}_{-1.2}$	$0.07^{+0.03}_{-0.05}$	$(1.59 \pm 0.14) \times 10^{-9}$	0.08
XCOF Sample [4]	$1.09^{+0.07}_{-0.07}$	$4.44^{+1.80}_{-1.85}$	$0.21^{+0.03}_{-0.02}$	$(1.12 \pm 0.11) \times 10^{-9}$	0.11
Vikhlinin Chandra [4]	$0.77 \pm 0.1$	$-3.5^{+2.6}_{-2.7}$	$(0.0002 \pm 0.018)\%$	$(9.26 \pm 1.66) \times 10^{-10}$	0.14
Chan et al [3]	$0.72^{+0.06}_{-0.06}$	$-5.49^{+1.39}_{-1.39}$	$0.27^{+0.02}_{-0.02}$	$9.5 \times 10^{-10}$	0.18
Tian et al [2]	$0.51^{+0.04}_{-0.05}$	$-9.80^{+1.07}_{-1.08}$	$14.7^{+2.9}_{-2.8}\%$	$(2.02 \pm 0.11) \times 10^{-9}$	0.11

TABLE I: The best-fit values obtained for the Chandra sample of G17 along with those obtained for other cluster samples. We see that the acceleration scale we obtain from this sample is in agreement with results from previous RAR analysis with clusters and about an order of magnitude higher than that obtained for galaxies.

- Nature Astronomy **2**, 927 (2018), 1811.05882.
- [9] D. C. Rodrigues, V. Marra, A. Del Popolo, and Z. Davari, Nature Astronomy **4**, 134 (2020), 2002.01970.
- [10] V. Marra, D. C. Rodrigues, and Á. O. F. de Almeida, Mon. Not. R. Astron. Soc. **494**, 2875 (2020), 2002.03946.
- [11] S. S. McGaugh, P. Li, F. Lelli, and J. M. Schombert, Nature Astronomy **2**, 924 (2018).
- [12] P. Kroupa, I. Banik, H. Haggi, A. H. Zonoozi, J. Dabringhausen, B. Javanmardi, O. Müller, X. Wu, and H. Zhao, Nature Astronomy **2**, 925 (2018), 1811.11754.
- [13] Z. Chang and Y. Zhou, Mon. Not. R. Astron. Soc. **486**, 1658 (2019), 1812.05002.
- [14] Y. Zhou, A. Del Popolo, and Z. Chang, Physics of the Dark Universe **28**, 100468 (2020), 2008.04065.
- [15] B. Famaey and S. S. McGaugh, Living Reviews in Relativity **15**, 10 (2012), 1112.3960.
- [16] H. Desmond, Mon. Not. R. Astron. Soc. **464**, 4160 (2017), 1607.01800.
- [17] J. F. Navarro, A. Benítez-Llambay, A. Fattahi, C. S. Frenk, A. D. Ludlow, K. A. Oman, M. Schaller, and T. Theuns, Mon. Not. R. Astron. Soc. **471**, 1841 (2017), 1612.06329.
- [18] A. D. Ludlow, A. Benítez-Llambay, M. Schaller, T. Theuns, C. S. Frenk, R. Bower, J. Schaye, R. A. Crain, J. F. Navarro, A. Fattahi, et al., Phys. Rev. Lett. **118**, 161103 (2017), 1610.07663.
- [19] S. McGaugh, Galaxies **8**, 35 (2020), 2004.14402.
- [20] A. A. Dutton, A. V. Macciò, A. Obreja, and T. Buck, Mon. Not. R. Astron. Soc. **485**, 1886 (2019), 1902.06751.
- [21] A. Paranjape and R. K. Sheth, arXiv e-prints arXiv:2102.13116 (2021), 2102.13116.
- [22] L. S. The and S. D. M. White, Astron. J. **95**, 1642 (1988).
- [23] S. Seeram and S. Desai, Journal of Astrophysics and Astronomy **42**, 3 (2021).
- [24] S. Boran, S. Desai, E. O. Kahya, and R. P. Woodard, Phys. Rev. D **97**, 041501 (2018), 1710.06168.
- [25] K. Pardo and D. N. Spergel, Phys. Rev. Lett. **125**, 211101 (2020), 2007.00555.
- [26] P. A. R. Ade et al. (Planck), Astron. Astrophys. **594**, A27 (2016), 1502.01598.
- [27] K. Gopika and S. Desai, arXiv e-prints arXiv:2106.07294 (2021), 2106.07294.
- [28] S. W. Allen, A. E. Evrard, and A. B. Mantz, Ann. Rev. Astron. Astrophys. **49**, 409 (2011), 1103.4829.
- [29] A. A. Vikhlinin, A. V. Kravtsov, M. L. Markevich, R. A. Sunyaev, and E. M. Churazov, Physics Uspekhi **57**, 317-341 (2014).
- [30] V. Halenka and C. J. Miller, Phys. Rev. D **102**, 084007 (2020), 1807.01689.
- [31] K. Gopika and S. Desai, Physics of the Dark Universe **30**, 100707 (2020), 2006.12320.
- [32] C. L. Sarazin, Reviews of Modern Physics **58**, 1 (1986).
- [33] Y.-T. Lin, S. A. Stanford, P. R. M. Eisenhardt, A. Vikhlinin, B. J. Maughan, and A. Kravtsov, Astrophys. J. Lett. **745**, L3 (2012), 1112.1705.
- [34] S. Rahvar and B. Mashhoon, Phys. Rev. D **89**, 104011 (2014), 1401.4819.
- [35] H. Ebeling, A. C. Edge, H. Bohringer, S. W. Allen, C. S. Crawford, A. C. Fabian, W. Voges, and J. P. Huchra, Mon. Not. R. Astron. Soc. **301**, 881 (1998), astro-ph/9812394.
- [36] H. Ebeling, A. C. Edge, S. W. Allen, C. S. Crawford, A. C. Fabian, and J. P. Huchra, Mon. Not. R. Astron. Soc. **318**, 333 (2000), astro-ph/0003191.
- [37] H. Dahle, Astrophys. J. **653**, 954 (2006), astro-ph/0608480.
- [38] G. B. Poole, M. A. Fardal, A. Babul, I. G. McCarthy, T. Quinn, and J. Wadsley, Mon. Not. R. Astron. Soc. **373**, 881 (2006), astro-ph/0608560.
- [39] D. S. Hudson, R. Mittal, T. H. Reiprich, P. E. J. Nulsen, H. Andernach, and C. L. Sarazin, Astron. & Astrophys. **513**, A37 (2010), 0911.0409.
- [40] A. Vikhlinin, A. Kravtsov, W. Forman, C. Jones, M. Markevitch, S. S. Murray, and L. Van Speybroeck, Astrophys. J. **640**, 691 (2006), astro-ph/0507092.
- [41] S. Gupta and S. Desai, Classical and Quantum Gravity **36**, 105001 (2019), 1811.09378.
- [42] S. Gupta and S. Desai, Physics of the Dark Universe **28**, 100499 (2020), 1909.07408.
- [43] D. Foreman-Mackey, D. W. Hogg, D. Lang, and J. Goodman, Publ. Astron. Soc. Pac. **125**, 306 (2013), 1202.3665.
- [44] S. Hinton, C. Adams, , and C. Badger, *Samreary/chainconsumer v0.33.0* (2020), URL <https://doi.org/10.5281/zenodo.4280904>.

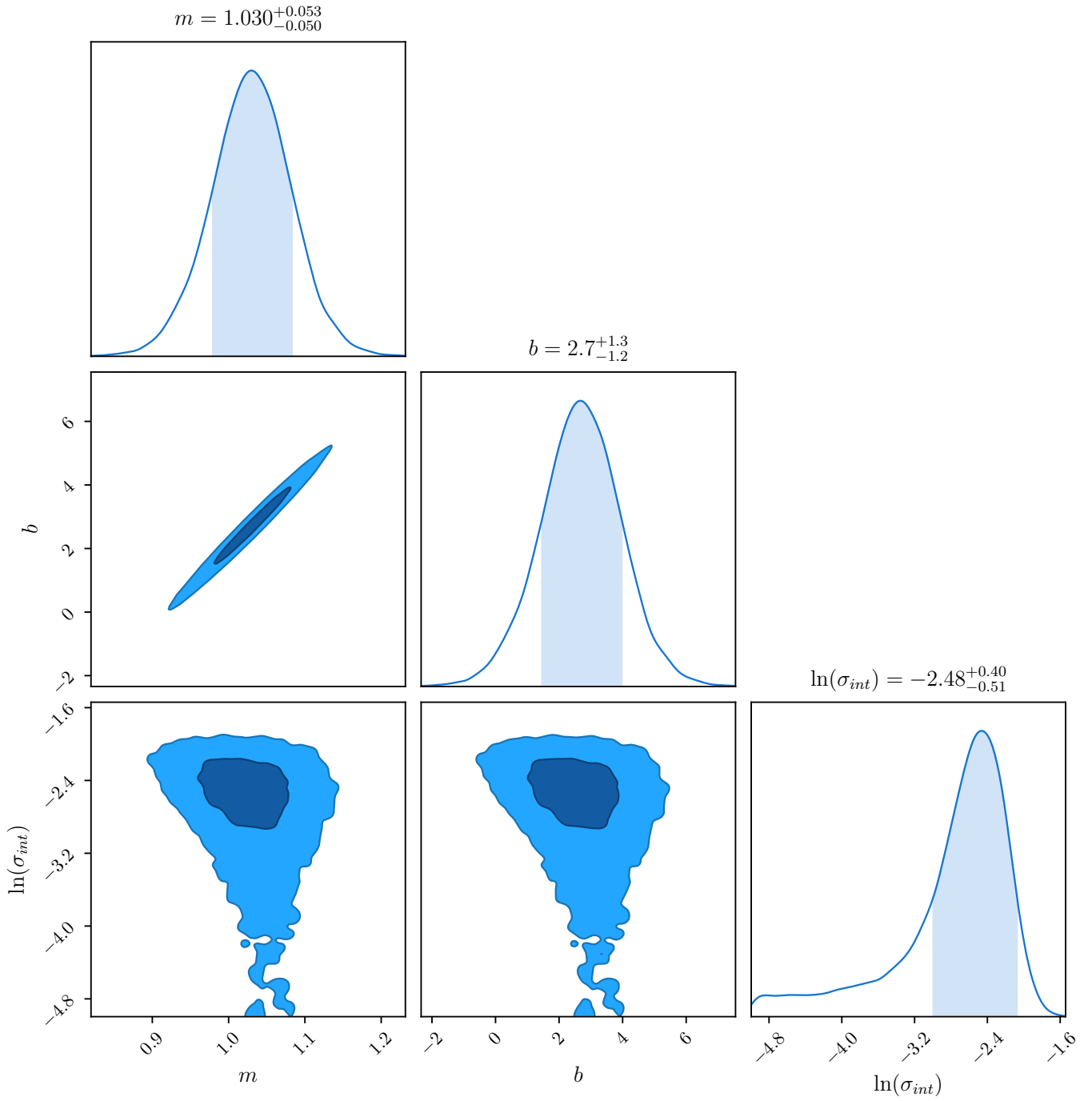


FIG. 2: 68% and 95% marginalized credible intervals obtained for the slope, intercept, and natural log of the intrinsic scatter on fitting the RAR to the Giles et al Chandra galaxy cluster sample [1].